NO-REFERENCE IMAGE SHARPNESS ASSESSMENT BASED ON LOCAL PHASE COHERENCE MEASUREMENT

Rania Hassen, Zhou Wang and Magdy Salama

Dept. of Electrical and Computer Engineering, University of Waterloo, Waterloo, Ontario, Canada
raniahassen@ieee.org, zhouwang@ieee.org, m.salama@ece.uwaterloo.ca

ABSTRACT

Sharpness is one of the most determining factors in the perceptual assessment of image quality. Objective image sharpness measures may play important roles in the design and optimization of visual perception-based auto-focus systems and image enhancement, restoration and compression algorithms. Here we propose a new sharpness measure where sharpness is identified as strong local phase coherence evaluated in the complex wavelet transform domain. Our test using the LIVE blur database shows that the proposed algorithm correlates well with subjective quality evaluations. An additional advantage of our approach is that other image distortions such as compression, median filtering and noise contamination that may affect perceptual sharpness can also be detected.

Index Terms— perceptual image quality, image sharpness, image blur, no-reference image quality assessment, local phase coherence, complex wavelet transform

1. INTRODUCTION

Humans are the ultimate consumers of almost all image and video products, but subjective image quality assessment is often costly, slow and difficult to be integrated into real-time image processing systems. Recently there has arisen an increasing need to develop objective visual quality measures that can automatically predict perceived image quality [1]. Many image quality measures require access to a distortion-free reference image, but in many real-world scenarios, the reference image does not exist or is unavailable. It is therefore important to develop no-reference measures that do not use any information about the reference image.

This work focuses on no-reference assessment of image sharpness, which is one of the most determining aspects of perceived image quality and can be affected by many types of image distortions. The most common ones are out-of-focus and motion blur, but other image distortions such as lossy compression, de-noising filtering, median filtering, and even noise contamination, could also affect perceived sharpness. The application scope of perceptual sharpness measures is beyond evaluating image quality, as they can be employed as design and optimization criteria in the development of visual perception-based auto-focus systems and image enhancement, restoration and compression algorithms.

In the literature, sharpness assessment is often equated with blurriness evaluation, as blur is the most common cause of the degradation of image sharpness. Both spatial and frequency transform domain methods have been proposed [2]. Spatial domain algorithms often rely on detecting the variations of global or local statistical features such as variance, autocorrelation, kurtosis, derivative energy and edge spread. Transform domain methods are mostly based on the fact that blur leads to energy attenuation at high spatial frequencies. The global or local frequency energy falloff can then be measured in different ways to identify image blur. An excellent review of many existing no-reference sharpness/blurriness metrics can be found in [2], where a spatial domain sharpness metric based on a novel concept of just-noticeable-blur (JNB) was proposed.

Following the idea in [3], here we examine image sharpness from a different perspective – local phase coherence (LPC), which states that the phases of complex wavelet coefficients exhibit a consistent relationship across scales in the vicinity of sharp image features, such as edges and lines. Specifically, we propose a new measure in this paper to quantify the degree of LPC at each spatial location. The LPC relationship is disrupted by a variety of image distortions that affect perceived sharpness, thus our measure can be used for sharpness assessment. Since our approach does not assume energy attenuation of high frequency components, it, to some extent, decouples sharpness and blurriness assessment. This distinguishes it from all existing transform domain methods.

2. LOCAL PHASE COHERENCE

The concept of local phase coherence can be better explained in one dimension. Given a signal $f(x)$ localized near the position x_0 where $f(x) = f_0(x - x_0)$, its wavelet transform can be written as:

$$F(s,p) = \int f(x) w^*_{s,p}(x) dx = \left[f(x) * \frac{1}{\sqrt{s}} g\left(\frac{x}{s}\right) e^{\jmath \omega_c x/s} \right]_{x=p} \quad (1)$$

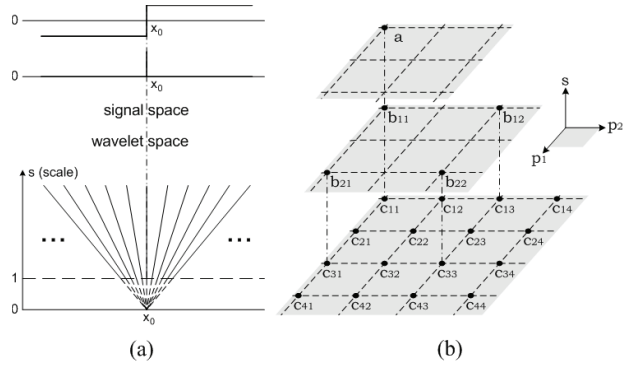

Fig. 1. (a) Local phase coherence of localized sharp feature at x_0; (b) 2D sampling grid of wavelet coefficients.

where $s \in R^+$ is the scale factor, $p \in R$ is the translation factor and the family of wavelets $w_{s,p}(x)$ is derived from the mother wavelet $w(x) = g(x)\, e^{j\omega_c x}$ (with center frequency ω_c and a slowly varying and symmetric envelop function $g(x)$):

$$w_{s,p}(x) = \frac{1}{\sqrt{s}}\, w\Big(\frac{x-p}{s}\Big) = \frac{1}{\sqrt{s}}\, g\Big(\frac{x-p}{s}\Big)\, e^{j\omega_c (x-p)/s}\,. \quad (2)$$

Using the convolution theorem, and the shifting and scaling properties of Fourier transform, Eq. (1) can be written as

$$\begin{aligned} F(s,p) &= \frac{1}{2\pi}\int_{-\infty}^{\infty} F(\omega)\sqrt{s}G(s\,\omega-\omega_c)e^{j\omega p}d\omega \\ &= \frac{1}{2\pi\sqrt{s}}\int_{-\infty}^{\infty} F_0\left(\frac{\omega}{s}\right)G(\omega-\omega_c)\, e^{j\omega(p-x_0)/s}d\omega\,, \end{aligned} \quad (3)$$

where $F(\omega)$, $F_0(\omega)$ and $G(\omega)$ are the Fourier transforms of $f(x)$, $f_0(x)$ and $g(x)$, respectively. The phase of $F(s,p)$ depends on the nature of $F_0(\omega)$. If $F_0(\omega)$ is scale invariant, meaning that $F_0(\omega/s) = K(s)F_0(\omega)$, where $K(s)$ is a real function of only s, but independent of ω, then we have

$$F(s,p) = \frac{K(s)}{\sqrt{s}} F(1, x_0 + \frac{p-x_0}{s})\,. \quad (4)$$

Analytically, the only type of scale-invariant continuous-spectrum signal follows a power law: $F_0(\omega) = K_0\,\omega^P$. In the spatial domain, the functions $f_0(x)$ that satisfy this condition includes the step function and its derivatives, which are precisely localized in space. Because $K(s)$ and s are both real, we obtain

$$\Phi(F(s,p)) = \Phi(F(1, x_0 + \frac{p-x_0}{s}))\,. \quad (5)$$

Eq. (5) suggests a strong phase coherence relationship across scale and space, where equal-phase contours in the (s,p) plane form straight lines (defined by $x_0 + (p-x_0)/s = C$, where C can be any constant) that converge exactly at the location of the feature x_0, as illustrated in Fig. 1(a).

The above results can be extended for two-dimensional signals or images [3], where the fine-scale coefficients can be well predicted from their coarser-scale neighboring coefficients, provided that the local phase satisfies the phase coherence relationship defined in Eq. (5). In the case that the positions of the neighboring complex wavelet coefficients are aligned as in Fig. 1(b), the phases of the finest scale coefficients $\hat{\Phi}(\{c_{ij}\})$ (for $i,j = 1,...,4$) can be predicted from coarser scale coefficients $\{a, b_{11}, b_{12}, b_{21}, b_{22}\}$ [3].

3. IMAGE SHARPNESS INDEX

Given an input image whose sharpness is to be evaluated, the proposed algorithm starts by constructing a spatially varying local phase coherence (LPC) map. The input image is decomposed into multi-orientation 3-scale subbands using the complex version of the steerable pyramid decomposition [4, 5]. We define a measure of LPC as

$$P_i = \frac{\sum_{l=1}^{L} |c_{i,l}| \cos\Big(\Phi\left(\{c_{i,l}\}\right) - \widehat{\Phi}\left(\{c_{i,l}\}\right)\Big)}{\sum_{l=1}^{L} |c_{i,l}| + K}\,, \quad (6)$$

where L is the number of orientations in the steerable pyramid decomposition, $\Phi\left(\{c_{i,l}\}\right)$ is the phase of the *i*-th coefficient in the finest subband of the *l*-th orientation, $\widehat{\Phi}\left(\{c_{i,l}\}\right)$ is the corresponding predicted phase, and K is a positive constant to avoid instability at small energy regions. This measure achieves the maximal value (capped by 1) when the phase prediction (and thus local phase coherence) is perfect. This is expected to occur in the vicinity of sharp image features such as ideal step edges. The measure is weighted by the magnitudes of the coefficients over orientations, so that the orientations that contain more energy are given higher importance. Figure 2(a) shows a natural image and its LPC map. It can be seen that the LPC measure responds strongly to sharp image structures around the central foreground region but weakly to the background out-of-focus regions. When the image is blurred as in Fig. 2(b), the strength of local phase coherence is reduced. Interestingly, slight reduction of LPC is also observed in the sharp regions when the image is contaminated by noise, as illustrated in Fig. 2(c).

In order to provide an overall evaluation about the sharpness of the image, we need to pool the LPC map into a single number of sharpness index. An interesting effect of subjective sharpness assessment is that humans tend to make their judgment based on the sharpest region in the image. For example, Fig. 2(a) is typically rated as a sharp image due to the sharp foreground region, regardless of the out-of-focus background area that appears to be very blurred. Such an effect suggests that pooling the LPC map by simple averaging would not result in a good overall metric, and a mechanism is necessary to put more emphasis on the sharpest regions in the image. Here we propose a weighted averaging method based on ranked LPC values: Let $\{P_i | i = 1, 2, \cdots, N\}$ be a collection of LPC values in the LPC map, and let $\{P_{(i)} | i = 1, 2, \cdots, N\}$ denote the sorted LPC values such that $P_{(1)} \le P_{(2)} \le \cdots \le P_{(N)}$.

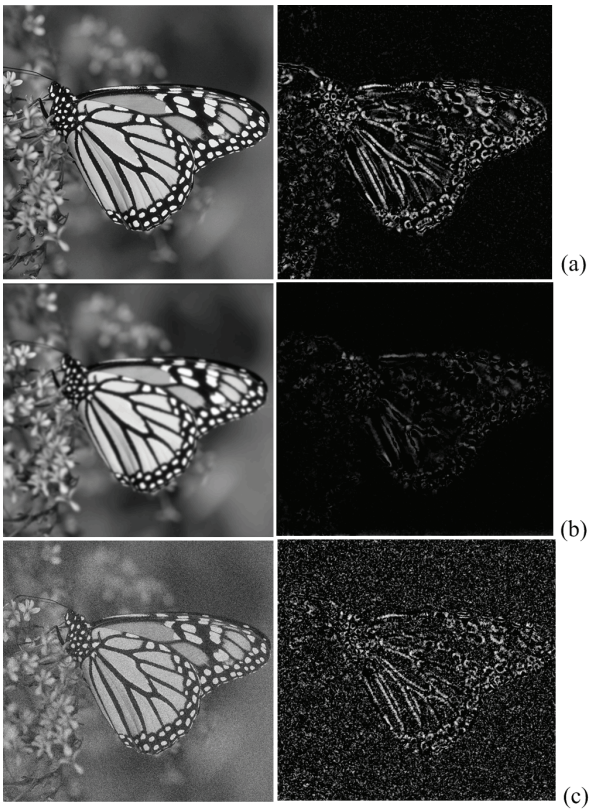

Fig. 2. Sample images and their LPC maps. (a) original image; (b) Blurred image; (c) noise contaminated image.

Then the overall image sharpness index (SI) is defined as

$$SI = \frac{\sum_{i=1}^{N} W_i \, P_{(i)}}{\sum_{i=1}^{N} W_i}, \tag{7}$$

where W_i is the weight assigned to the i-th ranked LPC value. W_i is given by

$$W_i = \exp\left[-\left(1 - \frac{i}{N}\right) \Big/ \beta \right], \tag{8}$$

which gives the highest LPC value a weight of 1. The weight decays exponentially as the rank goes down, and the speed of decaying is controlled by the parameter β.

A practical issue in the implementation of the proposed algorithm is that the LPC values computed near the four boundaries of the image are often significantly affected by these boundaries. This is largely due to the wide spread of the steerable pyramid filters. To avoid such boundary effects, we crop the boundary parts (by B pixels on each size of the four boundaries) of the LPC map and only use the central part to compute the SI. In all the experimental results reported in this paper, the parameters are set as $L = 4$, $K = 20$, $\beta = 0.0001$, and $B = 64$.

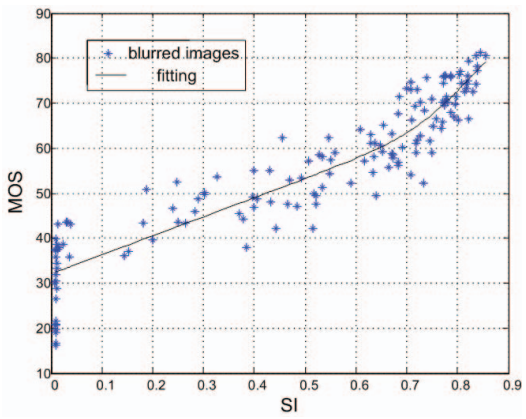

Fig. 3. Scatter plot of mean opinion score (MOS) versus SI model prediction of the blurred image dataset in LIVE database. Each data point represents one test image.

4. EXPERIMENTS

We first test the proposed sharpness index using the blur dataset in the publicly available LIVE database [6]. The dataset contains 174 images, including 145 blurred (using Gaussian filter of different sizes) and 29 reference images without blur. All images are rated by 20-25 subjects. For each image, the mean opinion score (MOS) and the standard deviation between subjective scores were recorded. Four metrics are computed for performance evaluation: 1) Spearman rank-order correlation coefficient (SROCC); 2) Pearson correlation coefficient (CC) after a nonlinear modified logistic mapping between the subjective and objective scores [6]; 3) Mean absolute error (MAE) between the true MOS and the model prediction of MOS; 4) Outlier ratio (OR), defined as the percentage of predictions outside the range of ± 2 standard deviations between subjective scores. Figure 3 shows the scatter plot between the objective and subjective scores together with the nonlinear fitting function. The quantitative evaluation results are given in Table 1, where the results are reported for two cases: full dataset (all 174 images) and blurred images only (145 images). The high SROCC and CC scores and low MAE and OR values indicate the high prediction accuracy, monotonicity and consistency of the proposed sharpness index. Comparisons with state-of-the-art JNB [2] and gradient-based [7] methods also demonstrates the superior performance of the proposed approach.

In the second experiment, we examine how the proposed sharpness index behaves when applied to a much wider range of image distortion types. In Fig. 4, we show a set of images, including an original sharp image, a noise contaminated image, a JPEG compressed image, a JPEG2000 compression image, a median filtered image and a Gaussian blurred image. By visual inspection, all distorted images exhibit certain degradations of perceptual sharpness, but to very

Table 1. Performance evaluation using LIVE blur dataset [6]

Model	Images	SROCC	CC	MAE	OR
JNB [2]	full set	0.8344	0.8497	6.9332	0.1322
Gradient [7]	full set	0.7625	0.8073	8.1892	0.2126
proposed	full set	0.9526	0.9439	4.3375	0.0460
JNB [2]	blurred	0.7821	0.8130	7.1118	0.1310
Gradient [7]	blurred	0.7147	0.7849	7.8900	0.1862
proposed	blurred	0.9368	0.9239	4.7681	0.0483

different degrees. Specifically, noise contamination indeed boosts the energy at high spatial frequencies (it also boosts low-frequency energy, but is negligible given the high power at low-frequencies in natural images), but still causes slight degradation of perceived sharpness. The block-DCT based JPEG compression reduces high-frequency energy within blocks, but create artificial high-frequencies at the block boundaries. Compared with JPEG, JPEG2000 compression avoids blocking effect, but looks more blurry. Both median and Gaussian filters strongly blur the image, but median filters are much better at preserving edges, and thus the image looks less blurry. Interestingly, the proposed sharpness index seems to correlate very well with our observations in all cases.

5. CONCLUSIONS

We propose a complex wavelet transform domain local phase coherence-based method for no-reference image sharpness assessment. Tests using the blur dataset in the LIVE database show that the proposed measure is well correlated with subjective scores. Perhaps the most distinguishing feature of the proposed approach from most existing methods is that it decouples sharpness and blurriness assessment. Instead of associating sharpness reduction with a blurring process, the degradation of sharpness is identified as the loss of local phase coherence. This leads to a novel sharpness measure that seems to respond reasonably to a much broader range of image distortion types, including compression, median filtering and noise contamination, which may or may not cause energy reduction at high spatial frequencies.

6. ACKNOWLEDGMENT

This work was supported in part by the Natural Sciences and Engineering Research Council of Canada in the form of Discovery and Strategic Grants, and in part by Ontario Ministry of Research & Innovation in the form of an Early Researcher Award, which are gratefully acknowledged.

Fig. 4. Proposed sharpness index (SI) applied to (a) original distortion-free image; (b) white Gaussian noise contaminated image; (c) JPEG compressed image; (d) JPEG2000 compressed image; (e) Median filtered image; (f) Gaussian blurred image.

7. REFERENCES

[1] Z. Wang and A. C. Bovik, *Modern Image Quality Assessment*, Morgan & Claypool Publishers, Mar. 2006.

[2] R. Ferzli and L. J. Karam, "A No-Reference Objective Image Sharpness Metric Based on the Notion of Just Noticeable Blur (JNB)," *IEEE Trans. Image Processing*, vol. 18, no. 4, pp. 717–728, 2009.

[3] Z. Wang and E. P. Simoncelli, "Local phase coherence and the perception of blur," *in Adv. Neural Information Processing Systems (NIPS03)*, pp. 786–792, 2004.

[4] E. P. Simoncelli, W. T. Freeman, E. H. Adelson, and D. J. Heeger, "Shiftable multi-scale transforms," *IEEE Trans. Info. Theory*, vol. 38, no. 2, pp. 587–607, Mar 1992.

[5] J. Portilla and E. P. Simoncelli, "A parametric texture model based on joint statistics of complex wavelet coefficients," *International Journal of Computer Vision*, vol. 40, pp. 49–71, 2000.

[6] H. R. Sheikh, M. F. Sabir, and A. C. Bovik, "A statistical evaluation of recent full reference image quality assessment algorithms," *IEEE Trans. Image Processing*, vol. 15, no. 11, pp. 3440–3451, 2006.

[7] X. Zhu and P. Milanfar, "A no-reference sharpness metric sensitive to blur and noise," in *1st International Workshop on Quality of Multimedia Experience (QoMEX)*, 2009.